Electrostatic Interactions between Peptides and the Molecular Chaperone DnaK

W. Liu,† D. Bratko,† J. M. Prausnitz,†,‡ and H. W. Blanch*,†

Department of Chemical Engineering, University of California, Berkeley, California 94720, and Chemical Sciences Division, Lawrence Berkeley National Laboratory, Berkeley, California 94720

Received: June 30, 2003

The molecular chaperone DnaK prevents intracellular protein misfolding and aggregation by transiently binding with newly synthesized polypeptides and protein-folding intermediates. DnaK preferentially binds to peptides with basic residues (Arg/Lys) present on the outside of a hydrophobic core. The electrostatic contribution toward DnaK/peptide binding was determined by measuring the dissociation constant of DnaK complexes with two fluorescein-labeled peptides (f-NRLLLTG and f-NALLLTG) using fluorescence anisotropy. The measured dissociation constants, K_d, differ significantly at low ionic strength: at 20 mM phosphate buffer; K_d for DnaK and f-NRLLLTG is 0.2 μM while that for DnaK and f-NALLLTG is 1 μM. This difference, attributed to stronger Coulombic binding in the case of f-NRLLLTG, vanishes at high ionic strength due to electrostatic screening. For f-NRAAATG, no interaction with DnaK was apparent, showing that hydrophobic interactions are essential in chaperone/peptide binding. The ionic strength dependence of the electrostatic interaction between DnaK and NRLLLTG is interpreted in terms of an approximate analytic model for the potential of mean force between DnaK and dipolar peptide. The calculated electrostatic binding free energy, ΔG_{ele}, of about −1 kcal/mol, is in good agreement with the experiment result for low salt concentration, as obtained from the ionic strength dependence of the measured dissociation constants. Our analytic model, here generalized to a pair of particles differing in size, charge, and dipole, provides a useful first estimate of electrostatic effects that can be exploited for control of protein−protein interactions.

I. Introduction

Molecular chaperones perform several functions including stabilizing newly synthesized polypeptides, translocating nascent protein chains, and refolding misfolded proteins.[1−3] DnaK is the Hsp70 (70 kDa heat-shock protein) molecular chaperone of *Escherichia coli*, containing a substrate-binding domain and an ATPase domain. Substrate binding and release are driven by switching between the low-affinity ATP-bound state and the high-affinity ADP-bound state.[4]

Interactions contributing to DnaK/substrate binding include hydrophobic forces, hydrogen bonds, van der Waals forces, electrostatic interactions, and structural factors (an arch formed by DnaK residues Met^{404} and Ala^{429} encloses peptide backbone in DnaK substrate-binding pocket).[5−9] A previous study of the substrate specificity of DnaK has shown that the binding motif of the peptide consists of a hydrophobic core of four to five residues enriched particularly in Leu and two flanking regions enriched in basic residues. Acidic residues are excluded from the core and disfavored in the flanking region. In folded proteins, these interaction sites are mostly buried and primarily found in the β-sheet region.[10−12]

Electrostatic forces often play a key role in protein−protein interactions. Interactions between groups of charged or polar residues located on protein surfaces can stabilize the protein−protein complex.[13] Protein aggregation and precipitation can also be driven by electrostatic forces.[14] The preference of DnaK to bind positively charged peptides indicates that electrostatic interactions enhance specific DnaK/substrate recognition, even though binding occurs in the DnaK hydrophobic pocket. Unlike hydrophobic interactions, electrostatic attraction is relatively easy to control by varying solution conditions such as pH and ionic strength. Control of electrostatic interactions therefore provides a powerful tool that can be exploited in the design and optimization of a variety of processes affected by interprotein binding. The goal of the present study is to elucidate the role of electrostatics in forming molecular chaperone/substrate complexes and to develop and test a simple analytic model that can provide a rapid first estimate of the electrostatic binding free energy for approximately globular, charged proteins with strong dipolar interactions.

We measured the dissociation constants for DnaK interacting with fluorescein-labeled peptides (f-NRLLLTG and f-NALLLTG) at several ionic strengths using fluorescence anisotropy.[15,16] The dissociation constant of ionized peptide f-NRLLLTG and DnaK showed a strong dependence on ionic strength. The binding strength of a nonionic peptide, f-NALLLTG, and DnaK showed no significant dependence on salt concentration and was similar to that for f-NRLLLTG and DnaK under screened electrostatic conditions. We obtain the electrostatic contribution to the free energy of DnaK/peptide binding from the difference between measured dissociation constants for DnaK and the two peptides at low and high ionic strengths. Experimental results are compared with the prediction of a simple analytic model for the electrostatic potential of mean force between DnaK and peptide NRLLLTG. The measured electrostatic free energy and the calculated contact value of the potential of mean force are in a good agreement, providing consistent estimates of the relative contributions from electrostatic and nonelectrostatic interactions in DnaK/peptide binding.

A variety of different theoretical methods are available to calculate the electrostatic free energy for a pair of protein

* Corresponding author: Tel (510) 642-1387; Fax (510) 643-1228; e-mail Blanch@socrates.berkeley.edu.
† University of California, Berkeley.
‡ Lawrence Berkeley National Laboratory.

10.1021/jp035872c CCC: $25.00
Published on Web 09/23/2003

molecules.[17−29] Typically, these methods rely on a dielectric continuum representation for the solvent.[30] The description of the interacting solutes, on the other hand, varies from the highly simplified hard-sphere approximation to nearly atomistic descriptions of the protein; an example of the latter is provided by the highly sophisticated DelPhi[19] and GRASP[20] computation packages. Application of these models is, however, computationally demanding and requires precise structural input for all interacting components, including information concerning conformational changes associated with the binding process. Even when using the best available structural information, free energy calculations may require arbitrary scaling procedures[31,32] that limit the validity of computed results to relative comparisons but do not always suffice for determination of absolute thermodynamic quantities of interest.

To provide a faster, albeit approximate, alternative, we consider a simplified model that represents protein and peptide molecules as roughly spherical particles with charge and with dipole moments.[29] The long-range protein/protein interaction is described by a DLVO-like theory, with screened charge and dipole interactions described by known analytic expressions based on the linearized Poisson−Boltzmann approximation.[17] The electrostatic potential of mean force between globular proteins is estimated as a sum of charge/charge and angle-averaged charge/dipole and dipole/dipole interactions,[17,21] augmented by a generalized expression for the coupling correction[29] which accounts for orientation probabilities that depend on all dipole-related interactions. Satisfactory agreement between the model prediction and the measured ionic-strength dependence of the electrostatic binding free energy between DnaK and peptide NRLLLTG illustrates the applicability of the proposed analytic approximation to estimate quantitatively electrostatic binding in protein solutions.

II. Materials and Methods

DnaK Production and Purification. The bacteria strain *E. coli* Top10 harboring plasmid pDnaK (a gift from Professor François Baneyx, the University of Washington) was employed for DnaK production. The cell culture and protein purification processes were performed according to procedures described in detail elsewhere.[33,34]

Bacteria were grown overnight at 30 °C in LB broth (10 g/L tryptone, 5 g/L yeast extract, and 5 g/L NaCl) and then incubated in a BiofloIII fermentor (New Brunswick Scientific, Edison, NJ) containing 1.5 L of supplemented LB medium (0.2% glucose and 34 μg/mL chloramphenicol). The cells were grown at 30 °C to the midexponential phase (absorbance at 600 nm, $A_{600} \approx 0.4$), induced with 1 mM IPTG, and were harvested at the late-exponential phase. The cell cultures were centrifuged at 8000*g* for 15 min at 0 °C, and the pellets were stored at −80 °C.

The frozen cell pellet (about 5 g wet weight) was resuspended in 20 mL of 10% sucrose in 50 mM Tris-HCl (pH 8.0) and disrupted using a French press at 10 000 psi. Soluble fractions were immediately clarified by centrifugation at 25 000*g* for 30 min at 0 °C. The supernatant was precipitated slowly by addition of saturated ammonium sulfate solution to 65% saturation. After slow stirring for 15 min at 0 °C, the mixture was centrifuged at 45 000*g* for 30 min at 0 °C. The protein pellet was slowly dissolved in buffer B (100 mM potassium phosphate, 100 mM ammonium sulfate, 5 mM mercaptoethanol, 5 mM EDTA, and 10% glycerol (v/v) at pH 7.0) and dialyzed against buffer B overnight.

The dialysate was chromatographed over a DE52-cellulose anion-exchange column (3 × 10 cm) (Whatman, Clifton, NJ) at a flow rate of 0.5 mL/min. After loading the protein sample, the column was washed with 2 column volumes of buffer B followed by buffer B-containing 500 mM NaCl. The relevant fraction was collected, dialyzed against buffer A (25 mM HEPES, 1 mM EDTA, 10 mM 2-mercaptoethanol, 10 mM NaCl and 3 mM $MgCl_2$, pH 8.0), and applied to an ATP-agarose column (1 × 7 cm) (Sigma, St. Louis, MO) at a flow rate of 0.5 mL/min. The column was washed with 10 volumes of buffer A and then with 10 volumes of buffer A-containing 500 mM NaCl. After equilibration of the column with 5 volumes of buffer A, DnaK protein was eluted with 10 column volumes of buffer A-containing 10 mM Mg-ATP (pH 7.6). The protein sample was dialyzed against TEN500 (20 mM Tris, 1 mM EDTA and 500 mM NaCl at pH 7.0) for 3 days with three buffer changes to remove free ATP.

The dialyzed sample was passed over a 1 mL Resource Q column (Pharmacia, Piscataway, NJ) followed by a TEN0 to TEN500 salt gradient elution over 20 mL at a flow rate of 0.5 mL/min. 10 μL aliquots of each collect were resolved on a 4−12% SDS-PAGE to determine the location of DnaK.

The resulting protein sample was dialyzed against TEN100 buffer for 2 days. The ratio of UV absorbance at wavelength 280 and 260 nm (A_{280}/A_{260}) was determined daily to monitor the removal of ATP (if $A_{280}/A_{260} > 1.5$, the solution was considered to be ATP free[35]). Protein concentration was determined by BCA (bicinchoninic acid)[36] protein assay (Pierce, Rockford, IL). Protein samples were stored at −80 °C.

Peptide Synthesis and Labeling. Three peptides (f-NRLLLTG, f-NALLLTG, and f-NRAAATG) were synthesized and fluorescein-labeled at N terminals by Dr. Michael Moore at the Cancer Research Center, University of California, Berkeley. Electrospray ionization mass spectrometry yielded peptide molecular weights consistent with those based on primary structures.

Fluorescence Anisotropy. Fluorescence anisotropy provides a method for measuring protein−protein interactions by observing the perturbations in the rotational molecular motion of fluorescent molecules. Because of Brownian motion, the molecular rotational diffusion coefficient D_r is[37,38]

$$D_r = \frac{RT}{6\eta V} \tag{1}$$

where R is the gas constant, T the absolute temperature, η the solution viscosity, and V the molecular volume. Upon association with other molecular species, the rotational motion of the fluorescent molecule changes because of the increase in its size. This effect can be related to fluorescence anisotropy, A, according to Perrin's equation:[15]

$$A = \frac{A_0}{1 + 6D_r\tau} \tag{2}$$

where A_0 is the limiting anisotropy representing the anisotropy in the absence of rotational molecular motion and τ is the fluorescence lifetime of the fluorophore.

Fluorescence anisotropy is measured by exciting a molecule with vertically polarized light and observing the fluorescence intensity of emitted light parallel to or perpendicular to the direction of polarization of the incident light. The anisotropy is obtained from these intensities by[15]

$$A = \frac{I_{||} - I_{\perp}}{I_{||} + 2I_{\perp}} \tag{3}$$

where I is the emitted light intensity measured along a direction parallel (||) or perpendicular ($\perp$) to the direction of excitation.

Consider binding interaction between two molecular species, P and L:

$$\mathrm{P} + \mathrm{L} \rightleftarrows \mathrm{PL} \tag{4}$$

P in this case represents molecular chaperone DnaK, and L denotes the fluorescent-labeled peptide. At equilibrium, the dissociation constant K_d can be expressed as

$$K_d = \frac{[\mathrm{P}][\mathrm{L}]}{[\mathrm{PL}]} \tag{5}$$

where [P], [L], and [PL] are the concentrations of DnaK, peptide, and DnaK−peptide complex, respectively.

When the concentration of DnaK is much higher than that of peptide in solution, the concentration [P] can be approximated by the total DnaK concentration [P_T]. The anisotropy is related to the dissociation constant by

$$A = A_f + (A_b - A_f)\left[\frac{[P_T]}{K_d + [P_T]}\right] \tag{6}$$

where A is the measured anisotropy in a mixture of free and bound fluorescent molecules with anisotropies A_f and A_b, respectively.[16]

The fluorescent-labeled peptides tumble at rates related to their molecular weight and volume and display modest anisotropy. However, when the peptides bind to much larger DnaK, their molecular rotation approaches that of DnaK, showing high anisotropy. During fluorescence anisotropy measurements, the fluorescent-labeled peptide concentrations were kept constant while the anisotropy was recorded as a function of increasing DnaK concentration.

Fluorescence Anisotropy Measurements. Fluorescence anisotropy measurements were performed using a BEACON 2000 (PanVera, Madison, WI) fluorescence−polarization system. The excitation wavelength was 495 nm, and the emission wavelength was 520 nm. A low volume (100 μL) chamber was used to minimize protein usage. Solutions of DnaK and peptides were incubated at 25 °C for 2 h to reach equilibrium. Figure 1 shows the anisotropy change associated with the binding of peptide f-NRLLLTG and f-NALLLTG with increasing concentrations of DnaK. The free peptide has an anisotropy value of 0.02 ± 0.002, while the anisotropy of DnaK-bound peptide reaches 0.08 ± 0.005 at the saturation region of the binding curve. The highest DnaK concentration used was around 10 μM (over 10−50K_d) where over 90% of peptide was bound to DnaK. The fluorescence intensity of peptide solutions was also recorded as a function of DnaK concentration and found to be constant (data not shown) during all measurements, suggesting that fluorescein does not bind with DnaK. To obtain dissociation constants, the anisotropy data were fitted to a first-order binding equation[16] using a regression algorithm from Sigma Plot.

Electrostatic Free Energy of Binding. To improve our ability to control interprotein interactions, it is useful to develop a model for approximate prediction of the electrostatic free energy of binding as a function of salt concentration and protein charges and protein dipole moments. Considering the electrostatic interactions to depend primarily on charge/charge, charge/dipole, and dipole/dipole terms, we apply a recent generalization of a DLVO-like model augmented with dipolar terms as discussed previously.[29] The model estimates the orientation-averaged potential of mean force between charged polar particles as a sum of independent charge/charge (qq), charge/dipole ($q\mu$), and dipole/dipole ($\mu\mu$) contributions,[17,21] corrected by a perturbation term[29] that accounts for the coupling between interdependent charge/dipole and dipole/dipole interactions. To date, this theoretical description has been applied only to a pair of identical proteins[29] where the perturbation term is always repulsive. To test the applicability of the model to our present system, below, we present a generalization to an asymmetric case, with interacting particles i and j carrying different charges, q_i, q_j, and dipole moments, μ_i, μ_j. This generalization leads to a new expression for the coupling perturbation term (eq 12) that may bring a qualitatively different effect of coupling between the three dipole-related contributions.

We begin our analysis by expressing the electrostatic potential of mean force $w_{ij}(r_{ij})$ as the sum of a direct charge/charge term, orientation averaged charge/dipole term[39] and dipole/dipole interaction term,[17,21] and perturbation $w_p(r_{ij})$:[29]

$$w_{ij}(r_{ij}) = u_{q_iq_j}(r_{ij}) + w_{q_i\mu_j}(r_{ij}) + w_{\mu_iq_j}(r_{ij}) + w_{\mu_i\mu_j}(r_{ij}) + w_p(r_{ij}) \tag{7}$$

where

$$u_{q_iq_j}(r_{ij}) = \frac{q_iq_j}{4\pi\epsilon\epsilon_0 r_{ij}} S_0(r_{ij},\kappa) \tag{8}$$

$$w_{q_i\mu_j}(r_{ij}) = -k_BT \ln\left[\frac{1}{\alpha_{ij}^{\,1}(r_{ij})} \sinh \alpha_{ij}^{\,1}(r_{ij})\right],$$

$$\alpha_{ij}^{\,1}(r_{ij}) = \frac{q_i\mu_j}{4\pi\epsilon\epsilon_0 r_{ij}^{\,2} k_BT} S_1(r_{ij},\kappa)$$

$$w_{\mu_iq_j}(r_{ij}) = -k_BT \ln\left[\frac{1}{\alpha_{ji}^{\,1}(r_{ij})} \sinh \alpha_{ji}^{\,1}(r_{ij})\right],$$

$$\alpha_{ji}^{\,1}(r_{ij}) = \frac{q_j\mu_i}{4\pi\epsilon\epsilon_0 r_{ij}^{\,2} k_BT} S_1(r_{ij},\kappa) \tag{9}$$

and

$$w_{\mu_i\mu_j}(r_{ij}) = -k_BT\left[\frac{2\alpha_{ij}^{\,2}(r_{ij})^2 + \alpha_{ij}^{\,3}(r_{ij})^2}{9}\right],$$

$$\alpha_{ij}^{\,2}(r_{ij}) = \frac{\mu_i\mu_j}{4\pi\epsilon\epsilon_0 r_{ij}^{\,3} k_BT} S_2(r_{ij},\kappa),$$

$$\alpha_{ij}^{\,3}(r_{ij}) = \frac{\mu_i\mu_j}{4\pi\epsilon\epsilon_0 r_{ij}^{\,3} k_BT} S_3(r_{ij},\kappa) \tag{10}$$

In these equations, r_{ij} is the center-to-center distance between the two particles, ϵ is the dielectric constant of the solvent, and ϵ_0 is the permittivity of vacuum; k_BT is the thermal energy, and $S_k(r_{ij},\kappa)$ stands for screening functions[17] for charge/charge (k = 0), charge/dipole (k = 1), and dipole/dipole (k = 2, 3) interactions given by eqs 4−7 of ref 29. In addition to the distance, r_{ij}, these functions depend on the Debye screening parameter $\kappa^2 = (2e_0^2N_AI)/(k_BT\epsilon_0\epsilon)$, where N_A is Avogadro's number, e_0 is the proton charge, $I = {}^1/_2\sum c_iz_i^2$ is the ionic strength of the solution,[30] and ϵ_p is the dielectric constant of the solute interior. The coupling correction $w_p(r_{ij})$ is estimated according to the discrete orientation model introduced in ref 29. The model considers only six principal orientations of the dipoles, giving a partition function with 36 angle-dependent contributions. For two identical particles, the symmetry of the model leads to a degeneracy that reduces the number of independent energy levels

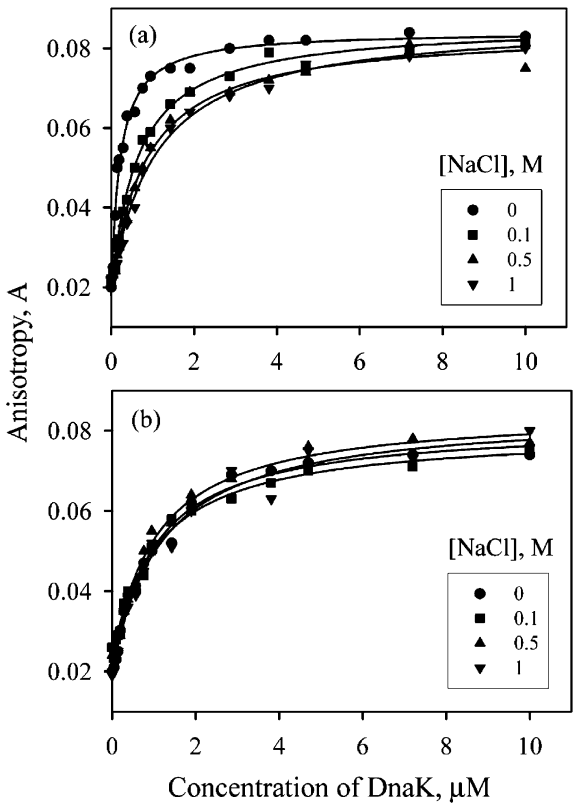

Figure 1. Fluorescence anisotropy measurements. The anisotropy, *A*, is measured as a function of DnaK concentration in 20 mM phosphate buffer at pH 7 and various NaCl concentrations. The fluorescence-labeled peptide concentration was 10 nM; (a) f-NRLLLTG, (b) f-NALLLTG. Symbols represent experimental data. Solid lines represent the best-fit curves using eq 6.

to eight. In the more general scenario ($\alpha_{ij}^1 \neq \alpha_{ji}^1$) considered in this work, the number of different energy levels is increased to 11. Following the analysis of ref 29, we obtain $w_d(r_{ij})$, the discrete orientation approximation to $w_{ij}(r_{ij})$:

$$w_d(r_{ij}) = u_{q_iq_j}(r_{ij}) - k_BT \ln[8 + 4e^{\alpha_{ij}^1} + 4e^{-\alpha_{ij}^1} + 4e^{\alpha_{ji}^1} + 4e^{-\alpha_{ji}^1} + 4e^{\alpha_{ij}^3} + 4e^{-\alpha_{ij}^3} + e^{-2\alpha_{ij}^2-(\alpha_{ij}^1-\alpha_{ji}^1)} + e^{2\alpha_{ij}^2-(\alpha_{ij}^1+\alpha_{ji}^1)} + e^{2\alpha_{ij}^2+(\alpha_{ij}^1+\alpha_{ji}^1)} + e^{-2\alpha_{ij}^2+(\alpha_{ij}^1-\alpha_{ji}^1)}] \quad (11)$$

We use eq 11 to obtain the coupling correction $w_p(r_{ij})$:

$$w_p(r_{ij}) = w_d(r_{ij},\alpha_{ij}^1,\alpha_{ji}^1,\alpha_{ij}^2,\alpha_{ij}^3) - w_d(r_{ij},0,0,\alpha_{ij}^2,\alpha_{ij}^3) - w_d(r_{ij},\alpha_{ij}^1,\alpha_{ji}^1,0,0) = -k_BT \ln(\{18[4 + 4\cosh\alpha_{ij}^1 + 4\cosh\alpha_{ji}^1 + 4\cosh\alpha_{ij}^3 + e^{-2\alpha_{ij}^2}\cosh(\alpha_{ij}^1 - \alpha_{ji}^1) + e^{2\alpha_{ij}^2}\cosh(\alpha_{ij}^1 + \alpha_{ji}^1)]\}/\{[8 + 4\cosh\alpha_{ij}^1 + 4\cosh\alpha_{ji}^1 + \cosh(\alpha_{ij}^1 - \alpha_{ji}^1) + \cosh(\alpha_{ij}^1 + \alpha_{ji}^1)][12 + 4\cosh\alpha_{ij}^3 + 2\cosh(2\alpha_{ij}^2)]\}) \quad (12)$$

For a symmetric case, $\alpha_{ij}^1 = \alpha_{ji}^1$, eq 12 simplifies to eq 21 of ref 29 applicable to identical interacting particles. In the latter case, with both proteins carrying charges of the same sign, the coupling correction is always repulsive because charge/dipole and dipole/dipole interactions favor opposite orientations. In a more general scenario, when the two charges may be of opposite signs, e.g., for the DnaK/peptide binding considered here, the two types of interaction can enhance each other, leading to stronger binding than that predicted by the conventional additivity approximation.[21] In the following section, we use the complete version of eq 7, including the coupling term given by eq 12, to estimate the measured electrostatic binding free energies.

The charges and dipole moments of the protein and peptide used in the calculation were taken from the online Weizmann Institute database,[40] based on protein crystal structures from the Protein Data Bank (PDB) and using the Parse set of partial atomic charges at pH 7.[5,41−43] Molecular volumes are obtained from the crystal structure data for the DnaK substrate-binding domain complex with peptide NRLLLTG from PDB.[5] The DnaK substrate-binding domain carries total charge $-10e_0$ and dipole moment 542 D. The peptide NRLLLTG has total charge $+1e_0$ and dipole moment 140 D. In our calculations, we determine the electrostatic free energy of binding as the electrostatic contribution to the potential of mean force between DnaK and peptide molecules at contact, that is, when $r_{12} = \sigma_{12} = (\sigma_1 + \sigma_2)/2$. In view of the deviation of molecular shapes for both DnaK and peptide from spherical geometry, molecular diameters, σ_1 and σ_2, were approximated by the diameters of equivalent spheres, i.e., spheres whose volumes are equal to those of the DnaK and the peptide molecules, respectively. This procedure leads to the effective sizes $\sigma_1 = 1.6$ nm for the peptide and $\sigma_2 = 4$ nm for the DnaK substrate binding domain; however, the precise DnaK/peptide contact distance can be considered an adjustable parameter of the model.

The DnaK ATPase domain is not involved in substrate binding directly and has little effect on the electrostatic interaction, but may increase the overall excluded volume. Including the volume of ATPase domain[44] increases the effective DnaK diameter to 5 nm. As shown below, the latter value leads to better agreement between calculated and measured electrostatic free energies of DnaK/NRLLLTG binding. The increase in the effective contact distance may also partly be attributed to the presence of the dye (fluorescein) attached to the peptide. Analogous to earlier studies,[45] our calculations presume no direct dye effect on peptide binding. Finally, a uniform dielectrict constant $\epsilon_p = 4$ was assigned to the interiors of interacting solutes.

III. Results and Discussion

Dissociation Constants and Determination of the Electrostatic Free Energy of Binding. The dissociation constants for peptide f-NRLLLTG or peptide f-NALLLTG and DnaK were measured by fluorescence anisotropy in 20 mM phosphate buffer with NaCl concentration at 0, 0.1, 0.5, and 1.0 M with results shown in Figure 2. The interaction between peptide f-NRLLLTG and DnaK showed a strong dependence on ionic strength. In 20 mM phosphate buffer, dissociation constants increase from 0.2 ± 0.02 μM in the absence of sodium chloride to 1.0 ± 0.05 μM in 1 M sodium chloride due to electrostatic screening of Coulombic attraction.

By substituting Arg with Ala in peptide f-NALLLTG, we eliminate the net positive charge on the peptide. The resulting dissociation constant for the f-NALLLTG/DnaK complex showed only a weak dependence on ionic strength because the primary interaction is hydrophobic, with binding strength very close to that of f-NRLLLTG with DnaK in the high-ionic-strength solution. This result confirmed that the electrostatic interaction between f-NRLLLTG and DnaK was completely screened in 1 M sodium chloride. Measurements for NALLLTG and DnaK also indicate that hydrophobic interaction is not appreciably affected by the presence of salt.

Like f-NRLLLTG, the peptide f-NRAAATG carries a single positive charge and is expected to exhibit a similarly strong

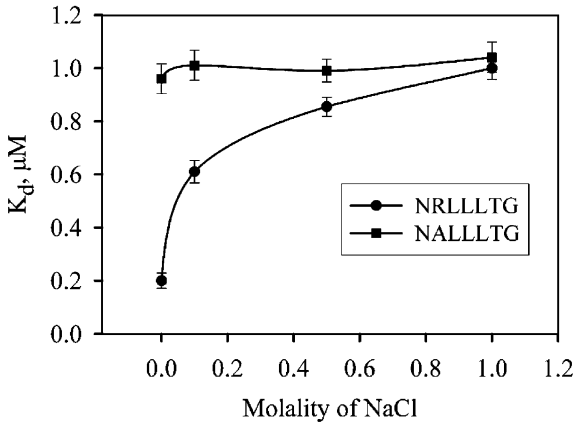

Figure 2. Dissociation constants for f-NRLLLTG and f-NALLLTG/DnaK complexes as a function of NaCl concentration in 20 mM phosphate buffer at pH 7. Lines are to guide the eye.

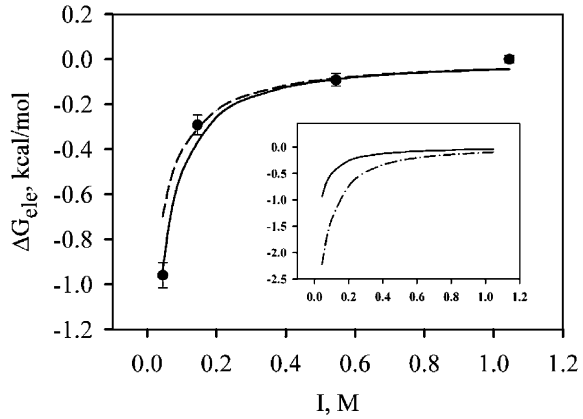

Figure 3. Comparison of ionic strength dependence of the electrostatic free energy, ΔG_{ele}, calculated from the additivity approximation (dashed line), from the present model with charge−dipole coupling (solid line), and from dissociation constant measurements (symbols). In these calculations, DnaK has a diameter of 5 nm, and the contact distance of DnaK/peptide is 3.3 nm. Inset: electrostatic free energy of binding from the approximate analytic model for DnaK with diameter 5 nm (solid line) and 4 nm (dash−dotted line) as a function of ionic strength *I*.

electrostatic interaction with DnaK. Substituting Leu residues by Ala, however, considerably reduces the hydrophobic character of the peptide. Fluorescence anisotropy data for f-NRAAATG revealed no binding to DnaK (data not shown), indicating the essential role hydrophobic interactions play in DnaK/peptide association.

Previous studies[5,6] have shown that the hydrophobic interaction is strongest between the Leu4 residue of the peptide and the DnaK substrate-binding pocket. This interaction is enhanced by hydrophobic contacts between Leu3,5 and DnaK. Arg also makes van der Waals contacts with the DnaK substrate-binding domain but in a less important manner. This is consistent with our finding that substitution of three Leucine residues in the peptide drastically reduces binding while this effect is not appreciable upon substitution of Arg with Ala.

From the dissociation constants for f-NRLLLTG and DnaK, the electrostatic binding free energy at weak screening −1.0 kcal/mol, using the relation $\Delta G_{ele} = RT \ln(K_{d2}/K_{d1})$, where K_{d2} and K_{d1} are the dissociation constants at high and low ionic strengths, respectively. The nonelectrostatic contribution (mainly hydrophobic interactions) was calculated from the dissociation constant at high ionic strength; it is −8.1 kcal/mol. In a previous study of the interaction between DnaK and acrylodan-labeled peptide NRLLLTG, the dissociation constant K_d was about 0.2 μM in the assay buffer of 25 mM Hepes/NaOH, 100 mM KCl, pH 7.0.[46] From our data, K_d for f-NRLLLTG with DnaK is about 0.2 ± 0.02 μM in 20 mM phosphate buffer and about 0.6 ± 0.05 μM in 20 mM phosphate buffer with 100 mM NaCl. Neither acrylodan nor fluorescein has any specific DnaK binding affinity.[45,46] It is not clear whether different types of salt ions present in the solution might cause the above discrepancy in dissociation constants.

Model Calculations. Figure 3 shows the ionic strength dependence of the electrostatic free energy of DnaK/NRLLLTG binding predicted by eqs 7−12 using the model parameters described above along with the effective DnaK/peptide contact distance σ_{12} = 3.3 nm (σ_2 = 5 nm) (solid curve). For comparison, Figure 3 includes a result based on the pairwise additivity approximation obtained by setting the coupling correction $w_p(\sigma_{12}) = 0$ (dashed curve). The shapes of both curves are consistent with the experimental electrostatic free energy (shown in symbols) obtained from dissociation constant measurements. The two curves in Figure 3 are almost indistinguishable at high screening, characterized by weak coupling between the distinct contributions, but differ by about 40% at low ionic strength ($I \sim 0.04$ M). This highlights the importance of the coupling term for accurate estimates of binding strengths when electrostatic interactions are not significantly reduced by screening. The coupling correction is attractive, in contrast to previously studied cases where both particles are either negatively or positively charged;[29] for such cases, the correction is always repulsive. In view of this distinction, an accurate account of the coupling term is crucial for predicting the outcome of a pH titration that brings about charge reversal on either of the interacting species.

Equations 8−10 predict a strong dependence of binding electrostatics on the contact distance of interacting molecules. The influence of the effective hard-sphere separation for a bound pair, σ_{12}, is shown in the inset of Figure 3 where we compare the ionic strength dependencies of the electrostatic free energy of binding for DnaK/NRLLLTG using the effective size of the entire DnaK molecule or the smaller value corresponding to the substrate-binding domain. In the former case (solid curve), σ_{12} = 3.3 nm, and in the latter case σ_{12} = 2.8 nm (dash−dotted curve). Comparison with the experimental dependence presented in Figure 3 shows excellent agreement between the experiment and theory when the higher σ_{12} is used. Both curves in the inset of Figure 3 reproduce qualitatively the ionic strength dependence observed experimentally.

The electrostatic potential surfaces of DnaK molecules surrounding the substrate-binding channel are electronegative on both sides and more negative on the binding site of the COOH-terminal group of the peptide NRLLLTG in the crystallized complex.[5,7] The polarity of such unfavorable binding alignment remains uncertain. Our potential of mean force model predicts that DnaK interacts more strongly with the peptide when a positively charged Arg residue is placed at a position closer to the N-terminus, resulting in a large dipole moment for the peptide. The calculated electrostatic binding energy, shown in Figure 4, is a strong function of peptide dipole moment, particularly at low ionic strength. This is reflected by noting that an increase in dipole moment of the peptide raises the dipole−dipole attraction to DnaK. This description emphasizes electrostatic interaction of the peptide with the global dipole moment of DnaK, not only with charges local to the binding site.

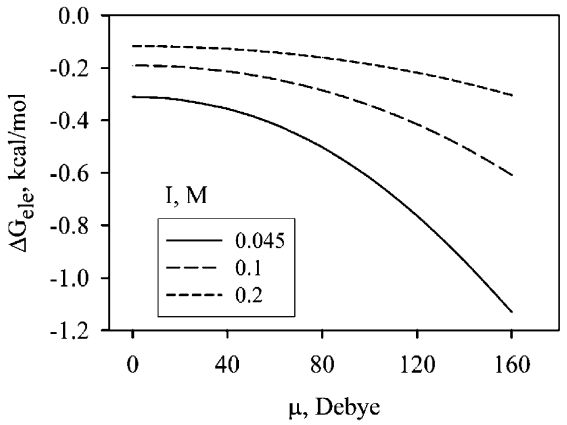

Figure 4. Calculation of electrostatic binding free energy, ΔG_{ele}, as a function of peptide dipole moment (μ) at different ionic strengths I. Dipole moments (relative to the center of mass) of stretched NRLLLTG, NLRLLTG, and NLLRLTG at pH = 7 are ~140, 123, and 105 D, respectively.

As different contributions to the total electrostatics (charge/charge, charge/dipole, and dipole/dipole) each feature a different ionic strength dependence,[17,29] the observed agreement with experiment suggests that our approximate model captures the essential contributions in correct proportions. At the expense of increased complexity, the angle averaging used in the model calculation can be improved by incorporating steric constraints imposed by the detailed protein geometry. However, the satisfactory performance of the simple model indicates that favorable orientations, dominating the weighted angle average of the electrostatic potential, are compatible with eventual steric restrictions in system under consideration here. Uncertainties associated with the appropriate value for the effective contact separation, σ_{12}, can be resolved by calibration, that is, by adjusting σ_{12} to reproduce the measured interaction strength at low salt concentration. Ignoring the presumably weak structural dependence on ionic strength or solution pH, the same apparent sizes can then be applied for calculations at different solution conditions or with another peptide of similar size. Applications of detailed models based on complete molecular geometries do not remove the need for similar calibrations.[18] Success of the simplified approach that considers only the leading electrostatic contributions, as illustrated in the above example, along with the advantage of computational simplicity, suggests that our generalization of the electrostatic model of ref 29 provides a viable tool toward obtaining useful first estimates of the strength of electrostatic binding between different protein/substrate pairs.

IV. Conclusions

Dnak recognizes peptides with internal hydrophobic residues and positively charged terminal residues.[5] To shed light on interactions between molecular chaperones and polypeptides, and especially to delineate the electrostatic contribution to their association, we determined the ionic strength dependence of dissociation constants for DnaK complexes with selected oligopeptides NRLLLTG, NRAAATG, and NALLLTG. The nonelectrostatic contribution to the free energies of binding between DnaK and ionic peptide NRLLLTG (determined from a comparison with electrostatically screened systems) agree with the corresponding value for the nonionic analogue of NRLLLTG, NALLLTG. While hydrophobic interaction dominates the chaperone/peptide interaction, the electrostatic contribution of -1.0 kcal/mol (close to $-2RT$) is sufficient to significantly affect the strength of association. Because we can easily modify interprotein electrostatics, e.g., by variation of ionic strength or pH, electrostatic interactions represent a promising tool to alter chaperone/peptide binding. To facilitate control of interprotein electrostatics, we have developed an approximate analytic model for prediction of the electrostatic contribution to the potential of mean force for a pair of dissimilar dipolar particles. For oppositely charged species, the model predicts a significant enhancement of interparticle attraction due to the cooperativity between charge/dipole and dipole/dipole interactions. The calculated electrostatic free energy of binding shows reasonable agreement with that obtained from fluorescence anisotropy measurements.

Acknowledgment. This work was supported by the National Science Foundation under Grant BES-0118208 and by the Office of Basic Energy Sciences of the U.S. Department of Energy. The authors thank Dr. Michael Moore for synthesis of peptides and Prof. François Baneyx for providing plasmid pDnaK.

References and Notes

(1) Fink, A. L. *Physiol. Rev.* **1999**, *79*, 425.
(2) Gething, M.; Sambrook, J. *Nature (London)* **1992**, *355*, 33.
(3) Hartl, F. U. *Nature (London)* **1996**, *381*, 571.
(4) Langer, T.; Lu, C.; Echols, H.; Flanagan, J.; Hayer, M. K.; Hartl, F. U. *Nature (London)* **1992**, *356*, 683.
(5) Zhu, X.; Zhao, X.; Burkholder, W. F.; Gragerov, A.; Ogata, C. M.; Gottesman, M. E.; Hendrickson, W. A. *Science* **1996**, *272*, 1606.
(6) Rüdiger, S.; Buchberger, A.; Bukau, B. *Nat. Struct. Biol.* **1997**, *4*, 342.
(7) Wang, H.; Kurochkin, A. V.; Pang, Y.; Hu, W.; Flynn, G. C.; Zuiderweg, E. R. P. *Biochemistry* **1998**, *37*, 7929.
(8) Tardieu, A.; Verge, A. L.; Malfois, M.; Bonneté, F.; Finet, S.; Riès-Kautt, M.; Belloni, L. *J. Cryst. Growth* **1999**, *196*, 193.
(9) Mayer, M. P.; Rüdiger, S.; Bukau, B. *J. Biol. Chem.* **2000**, *381*, 877.
(10) Fourie, A. M.; Sambrook, J. F.; Gething, M. H. *J. Biol. Chem.* **1994**, *269*, 30470.
(11) Gragerov, A.; Zeng, L.; Zhao, X.; Burkholder, W.; Gottesman, M. E. *J. Mol. Biol.* **1994**, *235*, 848.
(12) Rüdiger, S.; Germeroth, L.; Schneider-Mergener, J.; Bukau, B. *EMBO J.* **1997**, *16*, 1501.
(13) Sheinerman, F. B.; Norel, R.; Honig, B. *Curr. Opin. Struct. Biol.* **2000**, *10*, 153.
(14) Konno, T. *Biochemistry* **2001**, *40*, 2148.
(15) Lakowicz, J. R. *Principles of Fluorescence Spectroscopy*; Plenum Press: New York, 1983.
(16) Lundblad, J. R.; Laurence, M.; Goodman, R. H. *Mol. Endocrinol.* **1996**, *10*, 607.
(17) Phillies, G. D. J. *J. Chem. Phys.* **1974**, *60*, 2721.
(18) Gilson, M. K.; Sharp, K. A.; Honig, B. H. *J. Comput. Chem.* **1988**, *9*, 327.
(19) Nicholls, A.; Honig, B. *J. Comput. Chem.* **1991**, *12*, 435.
(20) Nicholls, A.; Sharp, K. A.; Honig, B. *Proteins: Struct. Funct. Genet.* **1991**, *11*, 281.
(21) Coen, C. J.; Blanch, H. W.; Prausnitz, J. M. *AIChE J.* **1995**, *41*, 996.
(22) Coen, C. J.; Newman, J.; Blanch, H. W.; Prausnitz, J. M. *J. Colloid Interface Sci.* **1996**, *177*, 276.
(23) McClurg, R. B.; Zukoski, C. F. *J. Colloid Interface Sci.* **1998**, *208*, 529.
(24) Sader, J. E.; Lenhoff, A. M. *J. Colloid Interface Sci.* **1998**, *201*, 233.
(25) Asthagiri, D.; Neal, B. L.; Lenhoff, A. M. *Biophys. Chem.* **1999**, *78*, 219.
(26) Farnum, M. A.; Zukoski, C. F. *Biophys. J.* **1999**, *76*, 2716.
(27) Neal, B. L.; Asthagiri, D.; Velev, O. D.; Lenhoff, A. M.; Kaler, E. W. *J. Cryst. Growth* **1999**, *196*, 377.
(28) Grant, M. L. *J. Phys. Chem. B* **2001**, *105*, 2858.
(29) Bratko, D.; Striolo, A.; Wu, J. Z.; Blanch, H. W.; Prausnitz, J. M. *J. Phys. Chem. B* **2002**, *106*, 2714.
(30) Friedman, H. L. *A Course in Statistical Mechanics*; Prentice Hall: Englewood Cliffs, NJ, 1985.
(31) Novotny, J.; Bruccoleri, R. E.; Davis, M.; Sharp, K. A. *J. Mol. Biol.* **1997**, *268*, 401.
(32) Kasper, P.; Christen, P.; Gehring, H. *Proteins: Struct. Funct. Genet.* **2000**, *40*, 185.
(33) Cegielska, A.; Georgopoulos, C. *J. Biol. Chem.* **1989**, *264*, 21122.

(34) Kamath-Loeb, A. S.; Lu, C. Z.; Suh, W.; Lonetto, M. A.; Gross, C. A. *J. Biol. Chem.* **1995**, *270*, 30051.
(35) Chaykin, S. *Biochemistry Laboratory Techniques*; Wiley: New York, 1966.
(36) Smith, P. K.; Krohn, R. I.; Hermanson, G. T.; Malia, A. K.; Gartner, F. H.; Provenzano, M. D.; Fujimoto, E. K.; Goeke, N. M.; Olson, B. J.; Klenk, D. C. *Anal. Biochem.* **1985**, *150*, 76.
(37) Einstein, A. *Ann. Phys.* **1906**, *19*, 371.
(38) Weber, G. *Adv. Protein Chem.* **1953**, *8*, 415.
(39) Miklavcic, S. J. *Phys. Rev. E* **1997**, *56*, 1142.
(40) http://bioinformatics.weizmann.ac.il/dipol.
(41) Felder, C. A.; Botti, S. A.; Lifson, S.; Silman, I.; Sussman, J. L. *J. Mol. Graphics Modell.* **1997**, *15*, 318.
(42) Botti, S. A.; Felder, C. E.; Sussman, J. L.; Silman, I. *Protein Eng.* **1998**, *11*, 415.
(43) Sitkoff, D.; Sharp, K. A.; Honig, B. *J. Phys. Chem.* **1994**, *98*, 1978.
(44) Flaherty, K. M.; DeLuca-Flaherty, C.; McKay, D. B. *Nature (London)* **1990**, *346*, 623.
(45) Montgomery, D. L.; Morimoto, R. I.; Gierasch, L. M. *J. Mol. Chem.* **1999**, *286*, 915.
(46) Pierpaoli, E. V.; Gisler, S. M.; Christen, P. *Biochemistry* **1998**, *37*, 16741.